



A microtopographic signature of life: Ecohydrologic feedbacks structure wetland microtopography

Jacob S. Diamond¹, Daniel L. McLaughlin¹, Robert A. Slesak², and Atticus Stovall³

¹School of Forest Resources and Environmental Conservation, Virginia Tech, Blacksburg, 24060, USA

5 ²Minnesota Forest Resources Council, St. Paul, 55108, USA

³NASA Goddard Space Flight Center, Greenbelt, 20771, USA

Correspondence to: Jacob S. Diamond (jacdia@vt.edu)



Abstract

Microtopography in wetlands can be a visually striking landscape feature, and also critically influences biogeochemical processes at both the scale of its observation (10^{-2} – 10^2 m²) and at aggregate scales (10^2 – 10^4 m²). However, relatively little is known about how microtopography develops in wetlands or the factors that influence its structure and pattern. For example, wetland vegetation appears to have a strong affinity to elevated microsites, but the degree to which wetland vegetation simply preferentially occupies elevated microsites (“hummocks”) versus the degree to which wetland vegetation reinforces and maintains these elevated microsites is not clear. Growing research across different ecosystems suggests that such reinforcing processes may be common between plants and their environment, resulting in self-organized patch features, like hummocks. Here, we made use of landscape ecology techniques and diagnostics to evaluate the plausibility of plant–environment feedback mechanisms in the maintenance of wetland microtopography. Using a novel terrestrial laser scanning dataset, we were able to quantify the sizing and spatial distribution of hummocks in 10 black ash (*Fraxinus nigra* Marshall) wetlands in northern Minnesota, U.S.A. We observed clear elevation bimodality in our wettest sites, indicating microsite divergence into two states: elevated hummocks and base elevation hollows. We coupled the TLS dataset to a three-year water table record and soil-depth measurements, and showed that hummock height is largely predicted by mean water table depth, with little influence of subsurface microtopography on surface microtopography. We further show that hummocks in wetter sites exhibit regular spatial patterning in contrast to hummocks in drier sites, which exhibit more random spatial arrangements. We show that hummock size distributions (perimeters, areas, and volumes) are lognormal, and that hummocks exhibit a characteristic patch area of approximately 1 m² across sites. Finally, we show that hummocks may be responsible for increased reactive surface area in black ash wetlands by up to 32%, and may also influence surface water dynamics through modulation of specific yield by up to 30%. We suggest that vegetation develops and maintains hummocks in response to anaerobic stresses from saturated soils, leading to a microtopographic signature of life.

Key words: hummocks, hollows, black ash, Fraxinus nigra, wetlands, ecohydrology, TLS

1 Introduction

Biota permeate the Earth’s surface, exerting direct control on surface processes and topographic features. Although topographic signatures of life at landscape scales remain elusive (Dietrich and Perron 2006), there is clear evidence of a biotic imprint on the land surface at the scale of biota (10^1 m; Lashermes et al., 2007, Roering et al., 2010), attributed to both animal (e.g., 1 m hill structures via burrowing; Gabet et al., 2014) and vegetative actions (e.g., 20–40 cm elevated ridges via organic inputs; Watts et al., 2010). Recently, vegetation’s role in affecting critical zone processes and resulting structure has received considerable research attention (Amundson et al., 2007, Reinhardt et al., 2010, Corenblit et al., 2011). However, despite general understanding of the broad, directional effects that vegetation imposes on the critical zone environment (e.g., bedrock weathering and soil development), less is known regarding the reciprocal feedbacks that develop between vegetation and their environment (Pawlik et al., 2016, Brantley et al., 2017). Some of these feedbacks may lead to reinforced and biotically maintained topographic structure (Eppinga et al., 2008), resulting in diagnostic (micro)topographic fingerprints of plants.



Microtopography, or the small-scale structured variation (10^{-1} – 10^0 m) in ground surface height, is common to many ecosystems. Wetland microtopography is particularly well studied, and is found in freshwater marshes (Van de Koppel
45 et al., 2006), fens (Sullivan et al., 2008), peat bogs (Nungesser 2003), forested swamps (Bledsoe and Shear 2000),
tidal freshwater swamps (Duberstein et al., 2013), and coastal marshes (Stribling et al., 2007). Wetland
microtopography is common enough that researchers in disparate systems collectively refer to local high points as
“hummocks” and local low points as “hollows”. Hollows are more frequently inundated and typically comprise large,
flat or concave open spaces, whereas elevated hummocks tend to be dispersed throughout hollows (Nungesser 2003,
50 Stribling et al., 2007). Elevated hummocks, even centimeters taller than adjacent hollows, can provide enough aeration
to limit anaerobic stress to vegetation, promoting higher plant abundance and primary production (Strack et al., 2006,
Rodríguez-Iturbe et al., 2007, Sullivan et al., 2008).

Microtopography changes the relative water table, affecting vegetative composition and growth in wetlands. However,
the degree to which wetland vegetation simply preferentially occupies hummocks (*sensu* Jackson & Caldwell 1996)
55 *versus* the degree to which wetland vegetation reinforces and maintains its own hummock microtopography (and thus
preferred environmental conditions) is not clear. For example, seedlings may simply fare better on elevated
microtopographic features such as downed woody debris or tree-fall mounds (Huenneke & Sharitz 1990). On the other
hand, increased vegetation root growth and associated organic matter inputs may support hummock expansion.
Growing research across different ecosystems suggests that such reinforcing processes, or feedback loops, may be
60 common between plants and their environment, and may result in characteristic, self-organized patch features
(Rietkerk and van de Koppel 2008). By quantifying the structure and patterning of these features, we may therefore
make process-based inferences about the latent feedback mechanisms (Turner 2005).

Several diagnostic features implicate feedback mechanisms in the reinforcement and maintenance of landscape
patches, like striping of vegetated patches in arid settings or maze-like patterns in mussel beds (Rietkerk and van de
65 Koppel 2008). We suggest that such diagnostic features from landscape ecology are extensible to wetland
microtopography, thereby allowing us to assess mechanisms of potential hummock self-organization. For example,
multimodal distributions in environmental variables, such as vegetation composition, soil texture, and, in our case,
elevation (and see Rietkerk et al., 2004, Eppinga et al., 2008, Watts et al., 2010), indicate patch self-organization
(Scheffer and Carpenter 2003). Hypothesized mechanisms for patch self-organization rely on positive feedbacks that
70 support so-called “local facilitation” (Pugnaire et al., 1996), where vegetation improves growth conditions locally by
modifying plant-scale soil properties (e.g., soil nutrients, hydraulic conductivity) or structure (elevation). This local
facilitation then leads to greater vegetation growth, further soil modification, and thus reinforced patch expansion.
However, this amplifying effect is ultimately constrained and stabilized by compensatory negative feedbacks (e.g.,
limiting nutrients, canopy competition for light; Rietkerk and van de Koppel 2008; Schröder et al., 2005). Negative
75 feedbacks can limit patch growth both vertically (in the case of elevation; Heffernan et al., 2013) and laterally,
constraining patch size. As such, patch size distributions may be used to query the scales at which coupled positive
and negative feedbacks operate.

Landscapes with a characteristic patch size imply that limits to patch growth operate at local, or patch scales (Manor
and Shnerb 2008, von Hardenberg et al., 2010). Limited patch growth results in a distinct absence of large patches,



80 and a truncation of the size distribution, which is modelled with lognormal or exponential functions (Kéfi et al., 2014, Watts et al., 2014). Characteristic patch sizes are also commonly accompanied by regular spatial patterning (Rietkerk et al., 2004), or spatial overdispersion of patches (i.e., uniformity of patch spacing is greater than expected by chance), which further implies local negative feedbacks to patch expansion (Watts et al., 2014). In contrast, patch size distributions may lack a characteristic spatial scale (e.g., Scanlon et al., 2007), which suggests a lack of scale-
85 dependent negative feedbacks to patch growth. Presence of very large patches characterize these scale-free patch size distributions, which are frequently modelled with power-law functions (Pascual and Guichard 2005). Here, we extend this inferential theoretical framework and specific diagnostics (multimodality, patch size distributions, and spatial patterning) to test predictions concerning the generation and maintenance of wetland microtopography.

Our broad hypothesis is that while there are many mechanisms that may initiate wetland microtopographic variation,
90 structured and persistent (and possibly patterned) wetland microtopography results from self-organizing, reciprocal feedbacks between plant growth and hydrology (Figure 1). Microtopographic initiation mechanisms may include direct actions from biota (e.g., burrowing or mounding), indirect actions from biota (e.g., tree falls or preferential litter accumulation), and abiotic events that redistribute soils and sediment (e.g., extreme weather events). However, without reinforcement, or autogenic feedbacks that maintain such variations in soil elevation, this type of microtopography
95 would be unstructured—indistinguishable from the random processes that create it, both vertically and laterally. On other hand, when operated on by autogenic feedbacks, these variations may take on a meaningful structure resulting from ecosystem processes.

Slightly elevated microsites provide relief from adverse hydrologically induced anaerobic conditions, promoting plant establishment. Plant establishment further leads to increased organic matter or sediment accumulation through several
100 potential mechanisms: 1) increased hummock gross primary productivity (GPP) and root growth from reduced hydrologic stress (Conner 1995, Stribling et al., 2007, Hanan and Ross 2009), 2) sediment/organic floc accumulation around stems, roots, and shoots during periods of inundation (Barry et al., 1996, Peterson and Baldwin 2004), and 3) a directional hydraulic and dissolved nutrient gradient towards hummocks driven by increased evaporation on hummocks relative to hollows, which leads to increased GPP on hummocks (hummock “evapoconcentration”;
105 Rietkerk et al., 2004, Eppinga et al., 2008). Thus, positive feedback loops develop where increased elevation induces greater plant productivity and sediment accumulation, which in turn lead to increased microsite elevation, and so on (top, solid loop in Figure 1).

These positive feedbacks ultimately induce soil elevation bimodality, where microtopographic features belong either to a stable hummock and stable hollow elevation state (Rietkerk et al., 2004, Eppinga et al., 2008, Watts et al., 2010).
110 Negative feedbacks eventually limit this growth; otherwise, hummocks would have no vertical or lateral limit. Vertical negative feedbacks may result from increased decomposition in hummocks as hummocks grow vertically and their soils become more aerobic (Courtwright and Findlay 2011; bottom, dashed loop in Figure 1). Lateral negative feedbacks may result from canopy competition for light among trees located on hummocks, or from competition for nutrients among hummocks (Rietkerk et al., 2004), leading to characteristic patch sizes and spatial overdispersion of
115 patches.



In wetlands, the posited positive and negative feedback loops that grow and maintain hummocks are likely under the strong influence of both site- and hummock-scale hydrology (blue shading in Figure 1). Consequently, we hypothesize that soil wetness is predictive of the strength of the autogenic processes that structure wetland microtopography. For example, drier sites may obviate the feedback loop between elevation and productivity/decomposition (*cf.* Watts et al., 2010), because soils are nearly always unsaturated and aerobic. Additionally, dissolved solutes may less easily flow along directional hydraulic routes in unsaturated soils compared to saturated soils, reducing the evapoconcentration effect. In contrast, we predict that in wetter sites both the elevation-productivity and evapoconcentration feedbacks will be more important, and will therefore lead to more clear and structured hummock-hollow features. In this framework, we view wetland hummocks as self-organizing, created autogenically by bidirectional feedbacks among vegetation, soil, and hydrology. Although our broad hypothesis has previously been tested in non-forested peatland environments (Belyea and Baird 2006, Eppinga et al., 2009), we seek here to expand and more directly quantify our understanding of the pattern and development of wetland microtopography in forested-wetland systems with a focus on hydrologic controls.

A potential null hypothesis of self-organizing, autogenic wetland microtopography is that hummocks and hollows are simply just reflections of similar undulations in some underlying soil horizon. The null hypothesis is easily tested through co-located measurements of surface soil horizon depth and underlying soil horizon topography. We would fail to reject this null hypothesis if we observe no correlation (slope = 0) between these variables, where surface soil depth is constant and thus surface microtopography is a reflection of subsurface microtopography. However, if we observe deviations from this no-correlation case, then we may reject this null hypothesis. This method therefore provides a litmus test of this first-order null hypothesis.

In this study, we assessed our self-organizing hummocks hypothesis by evaluating wetland soil elevations, hummock properties and patterning, and hydrologic regimes in black ash forested wetlands in northern Minnesota, U.S.A. To do so, we characterized microtopography with a 1-cm spatial resolution dataset from a terrestrial laser scanning campaign. We also evaluated subsurface mineral layer topography and daily water tables to determine the extent that these influenced observed surface microtopography. Specifically, we tested the following predictions:

1. Elevation will exhibit a bimodal distribution within black ash wetlands. A bimodal distribution of microtopography requires sharp boundaries between hummocks and hollows (Eppinga et al., 2009), which are indicative of positive feedbacks between biota and hummock growth (top feedback in Figure 1), and therefore suggest biotically controlled hummock development.
2. Surface soil depth will exhibit a -1:1 relationship with underlying mineral layer topography, but hummocks will plot above this line. In other words, hummocks and hollows are not simply reflections of the ups and downs of subsurface layers, but instead reflect surface-level self-organization of soil elevation.
3. Hummock heights will be positively correlated to site wetness. This prediction follows from the idea that hummocks are self-organizing, but only organize in response to elevated water tables. This prediction implies that drier sites may exhibit no microtopography because average water tables are low enough to where the feedbacks that support hummock expansion do not develop. Moreover, within-site variability in hydrology may also result in within-site variability in hummock heights.



- 155 4. Hummocks will be regularly spatial patterned. Regular spatial patterning requires coupling of scale-dependent positive and negative feedbacks (Rietkerk and van de Koppel 2008). Overdispersion and regular hummock spatial patterning may therefore arise when the increased local productivity on hummocks (i.e., local positive feedback as predicted in the previous hypothesis) inhibits the formation of hummocks at some distance away (e.g., canopy light and/or nutrient competition among trees on hummocks). However, we predict that regular patterning will only be clear in wetter sites with more pronounced microtopography (see 3 above).
- 160 5. Cumulative distribution (cdf) of individual hummock areas will correspond to a family of truncated distributions (e.g., exponential or lognormal). This type of patch-size distribution implies a characteristic patch size, and tends to emerge for patches that grow with local facilitation but also a local constraint that limits their maximum size (e.g., resource competition). We hypothesized that light and nutrients would be limiting to plant growth in these systems, both of which may act at the scale of hummocks, thus leading to
- 165 truncated hummock patch size distributions.

2 Methods

2.1 Site descriptions

To test our hypotheses, we investigated ten black ash (*Fraxinus nigra* Marshall) wetlands of varying size and hydrogeomorphic landscape position in northern Minnesota, U.S.A. (Figure 2; Table 1). Thousands of meters of sedimentary rocks overlay an Archean granite bedrock geology in this region. Study sites are located on a glacial moraine landscape (400–430 m ASL) that is flat to gently rolling, with the black ash wetlands found in lower landscape positions that commonly grade into aspen or pine-dominated upland forests. The climate is continental, with mean annual precipitation of 700 mm and a mean growing season (May–October) temperature of 14.3°C (mean annual temperature = -1.1°C – 4.8°C; WRCC 2019). Annual precipitation is approximately two-thirds rain and one-third snowfall. Potential ET (PET) is approximately 600–650 mm per year (Sebestyen et al., 2011). Detailed site histories were unavailable for the ten study wetlands, but silvicultural practices in black ash wetlands have been historically limited in extent (D’Amato et al., 2018). Based on the available information (e.g., Erdmann et al., 1987, Kurmis and Kim 1989), we surmise that our sites are late successional or climax communities and have not been harvested for at least a century.

180 As part of a larger effort to understand and characterize black ash wetlands (D’Amato et al., 2018), we categorized and grouped each wetland by its hydrogeomorphic characteristics as follows: 1) depression sites (“D”, n = 4) characterized by a convex, pool-type geometry with geographical isolation from other surface water bodies and surrounded by uplands, 2) lowland sites (“L”, n = 3) characterized by extensive wetland complexes on flat, gently sloping topography, and 3) transition sites (“T”, n = 3) characterized as flat, linear boundaries between uplands and black spruce (*Picea mariana* Mill. Britton) bogs (Figure 3). The three lowland sites were control plots from a long-term experimental randomized block design on black ash wetlands (blocks 1, 3, and 6; Slesak et al., 2014, Diamond et al., 2018). We considered hydrogeomorphic variability among sites an important criterion, as it allowed us to capture



expected differences in hydrologic regime and thus differences in the strength of our predicted control on microtopographic generation (Figure 1). Ground slopes across sites ranged from 0–1%. Hydrology of black ash wetlands is typically dominated by precipitation and evapotranspiration (ET), with shallow water tables following a common annual trajectory of late-spring/early-summer inundation followed by summer drawdown from ET (Slesak et al., 2014, Diamond et al., 2018). However, the degree of drawdown depends on local hydrogeomorphic setting; we observed considerably wetter conditions at depression sites and transition sites than lowland sites.

2.1.1 Vegetation

Overstory vegetation at the ten sites is dominated by black ash. At the lowland sites, other overstory species were negligible, but at the depression and transition sites there were minor cohorts of northern white-cedar (*Thuja occidentalis* L.), green ash (*Fraxinus pennsylvanica* Marshall), red maple (*Acer rubrum* L.), yellow birch (*Betula alleghaniensis* Britt.), balsam poplar (*Populus balsamifera* L.), and black spruce (*Picea mariana* Mill. Britton). Except at one transition site (T1), where northern white cedar represented a significant overstory component, black ash represented over 75% of overstory cover across all sites. Black ash also made up the dominant midstory component in each site, but was regularly found with balsam fir (*Abies balsamea* L. Mill.) and speckled alder (*Alnus incana* L. Moench) in minor components, and greater abundances of American elm (*Ulmus Americana* L.) at lowland sites. Black ash stands are commonly highly uneven-aged (Erdmann et al., 1987), with canopy tree ages ranging from 130–232 years, and stand development under a gap-scale disturbance regime (D’Amato et al., 2018). Black ash are also typically slow-growing, achieving heights of only 10–15 m and diameters at breast height of only 25–30 cm after 100 years (Erdmann et al., 1987).

2.1.2 Soils

Soils in black ash wetlands in this region tend to be Histosols characterized by deep mucky peats underlain by silty clay mineral horizons, although there were clear differences among site groups (NRCS 2019). Depression sites were commonly associated with Terric haplosaprists of the poorly drained Cathro or Rifle series with O horizons approximately 30–150 cm deep (Table 1). Lowland sites were associated with lowland Histic inceptisols of the Wildwood series, which consist of deep, poorly drained mineral soils with a thin O horizon (< 10 cm) underlain by clayey till or glacial lacustrine sediments. Transition sites typically had the deepest O horizons (> 100 cm), and were associated with typic haplosaprists of the Seelyeville series and Typic haplohemists (NRCS 2019). Both depression and transition sites had much deeper O horizons than lowland sites, but depression site organic soils were typically muckier and more decomposed than more peat-like transition site organic soils.

2.2 TLS

2.2.1 Data collection

To characterize the microtopography of our sites, we conducted a terrestrial laser scanning (TLS) campaign from October 20–24, 2017. We chose this period to ensure high-quality TLS acquisitions, as it coincided with the time of least vegetative cover and the least likelihood for inundated conditions. During scanning, leaves from all deciduous



canopy trees had fallen and grasses had largely senesced. Standing water was present at portions of three of the sites and was typically dispersed across the site in small pools (*ca.* 0.5–2 m²) less than 10 cm deep. We used a Faro Focus 120 3D phase-shift TLS (905 nm λ) to scan three randomly established, 10 m diameter sampling plots at each site (see 225 Stovall et al., [in revision] for exact methodological details). For each site, we merged our plot-level TLS data to a single ~900 m² site-level point-cloud using 30 strategically placed and scanned 7.62 cm radius polystyrene registration spheres set atop 1.2 m stakes. We referenced each site to a datum located at each site's base well elevation. We installed sixty 2.54 cm radius spheres on fiberglass stakes exactly 1.2 m above ground surface at each site to validate the TLS surface model products. With the validation locations we could easily calculate the exact surface 230 elevation (i.e., 1.2 m below a scanned sphere) of 60 points in space. We installed 39 (13 at each plot) validation spheres at points according to a random walk sampling design, and placed 21 (7 at each plot) validation spheres on distinctive hummock-hollow transitions. We placed the 1.2 m tall validation spheres approximately plumb to reduce errors due to horizontal misalignment. We processed the point clouds generated from the TLS sampling campaign to generate two products: 1) site-level 1 235 cm resolution ground surface models, and 2) site-level delineations of hummocks and hollows. The details and validation of this method are described completely in Stovall et al., (in review), but a brief summary is provided here.

2.2.2 Surface model processing and validation

For each site, we first filtered the site-level point-clouds in the CloudCompare software (Othmani et al., 2011) and created an initial surface model with the absolute minima in a moving 0.5 cm grid. We removed tree trunks from this 240 initial surface model using a slope analysis and implemented a final outlier removal filter to ensure all points above ground level were excluded. Our final site-level surface models meshed the remaining slope-filtered point cloud using a local minima approach at 1 cm resolution. We validated this final 1 cm surface model using the 60 validation spheres per site.

Before we analyzed surface models from each site, we first detrended sites that exhibited site-scale elevation gradients 245 (e.g., 0.02 cm m⁻¹). These gradients may obscure analysis of site-level relative elevation distributions (Planchon et al., 2002), and our hypothesis relates to relative elevations of hummocks and hollows and not their absolute elevations. We chose the best-detrended surface model based on adjusted R² values and observation of resultant residuals and elevation distributions from three options: no detrend, linear detrend, and quadratic detrend (P. Five sites were 250 detrended: L2 was detrended with a linear model, and D1, D2, D4, and T1 were detrended with quadratic models. We then subsampled each surface model to 10,000 points to speed up processing time as original surface models were approximately 100,000,000 points. We observed no significant difference in results from the original surface model based on our subsampling routine.

2.2.3 Hummock delineation and validation

We classified the final surface model into two elevation categories: hummocks and hollows. We first classified 255 hollows using a combination of normalized elevation and slope thresholds; hollows have less than average elevation and less than average slope. This combined elevation and slope approach avoided confounding hollows with the tops



of hummocks since the tops of hummocks are typically flat or shallow sloped. We removed hollows and used the remaining area as our domain of potential hummocks.

260 Within the potential hummock domain, we segmented hummocks into individual features using a novel approach –
TopoSeg (Stovall et al., in revision) – and thereby created a hummock-level surface model for each site. We first used
the local maximum (Roussel and Auty, 2018) of a moving window to identify potential microtopographic structures
for segmentation. The local maximum served as the “seed point” from which we then applied a modified watershed
delineation approach (Pau et al., 2010). The watershed delineation inverts convex topographic features and finds the
edge of the “watershed”, which in our case are hummock edges. The defined boundary was used to clip and segment
265 hummock features into individual hummock surface models.

For each delineated hummock within all sites, we calculated perimeter length, total area, volume, and height
distributions relative both to local hollow datum and to a site level datum. To calculate area, we summed total number
of points in each hummock raster multiplied by the model resolution (1 cm²). We calculated volume using the same
method as area, but multiplied by each points’ height above the hollow surface. Perimeter was conservatively
270 estimated by converting our raster-based hummock features into polygons and extracting the edge length from each
hummock. We estimated side hummock area (analogous to the surface area of a cylinder without a top or bottom) by
multiplying the perimeter of each hummock by its 20th percentile height, which we determined to be a conservative
representation of the average height around the perimeter of the hummock.

To validate the hummock delineation, we compared manually delineated and automatically delineated hummock size
275 distributions at one depression site (D2) and one transition site (T1), both with clearly defined hummock features. We
omitted using a lowland site for validation because none of these sites had obvious hummock features that we could
manually delineate with confidence. We manually delineated hummocks for the D2 and T1 sites with a qualitative
visual analysis of raw TLS scans using the clipping tool in CloudCompare (2018). Stovall et al., (2019) found no
significant differences between the manual and automatically segmented hummock distributions and feature geometry
280 had an RMSE of less than ~20%.

After the automatic delineation procedure and subsequent validation, we performed a data cleaning procedure by
manually inspecting outputs in the CloudCompare software. We eliminated clear hummock mischaracterization that
was especially prevalent at the edges of sites, where point densities were low. We also excluded downed woody debris
from further hummock analysis because, although these features may serve as nucleation points for future hummocks,
285 they are not traditionally considered hummocks and their distribution does not relate to our broad hypotheses. Finally,
we excluded delineated hummocks that were less than 0.1 m² in area because we did not observe hummocks less than
this size during our field visits. This delineation and manual cleaning process yielded point clouds of hummocks and
hollows for every site that could be further analyzed.

2.2.4 Surface model performance

290 Validation of surface models using the validation spheres indicated that surface models were precise (RMSE = 3.67
± 1 cm) and accurate (bias = 1.26 ± 0.1 cm) across all sites (Stovall et al., in revision). The gently sloping lowland
sites (L) had substantially higher RMSE and bias than the transition (T) and depression (D) sites. The relatively high



error of lowland site validation points resulted from either low point density or a complete absence of LiDAR returns. We observed overestimation of the surface model when TLS scans were unable to reach the ground surface, leading to the greatest overestimations in sites with dense grass cover (lowland sites). Overestimation was also common in locations with no LiDAR returns, such as small hollows, where the scanner's oblique view angle was unable to reach. Nonetheless, examination of the surface models indicated clear ability of the TLS to capture surface microtopography (Figure S1).

2.2.5 Hummock delineation performance

Hummocks delineated from our algorithm were generally consistent in distribution and dimension with manually delineated hummocks. However, the automatic delineation located hundreds of small ($<0.1 \text{ m}^2$) "hummock" features that were not captured with manual delineation, which we attribute to our detrending procedure. We did not consider automatically delineated hummocks less than 0.1 m^2 in further analyses, as we did not observe hummocks smaller than this in the field. Both area and volume size distributions from the manual and automatic delineations were statistically indistinguishable for both t-test (p-value = 0.84 and 0.51, respectively) and Kolmogorov-Smirnov test (p-value = 0.40 and 0.88, respectively). Automatically delineated hummock area, perimeter:area, and volume estimates had 23%, 19.6%, and 24.1% RMSE, respectively, and the estimates were either unbiased or slightly negatively biased (-9.8 %, 0.2 %, and -11.9 %, respectively). We consider these errors to be well within the range of plausibility, especially considering the uncertainty involved in manual delineation of hummocks, both in the field and on the computer. Final delineations showed clear visual differences among site types in the spatial distributions of hummocks (Figure S2).

2.3 Field data collection

2.3.1 Mineral layer depth measurements

To quantify the control that underlying mineral layer microtopography has on surface microtopography, we conducted synoptic measurements of mineral layer depth and thus organic soil thickness at each site. Within each of the 10 m diameter plots used for TLS at each site, we took 13 measurements (co-located with the randomly established validation spheres) of depth to mineral layer using a steel 1.2 m rod. At each point the steel rod was gently pushed into the soil with consistent pressure until resistance was met – we performed this resistance test twice at each point and recorded the average depth until resistance (resolution = 1 cm) as the depth to mineral layer. At nearly every point, there was a clear difference in resistance when a mineral layer was reached. In cases where it was unclear whether the steel rod reached a mineral layer (e.g., hitting a tree root), three measurements were taken in the surrounding 50 cm region and averaged. Later, we tied each of these depth-to-mineral-layer measurements with a soil elevation based on TLS data and the site-level datum (i.e., elevation at the base of each site's well, see Data collection).

2.3.2 Hydrology

To address our hypothesis that hydrology is a controlling variable of microtopographic expression in black ash wetlands, we instrumented all 10 sites to monitor water level dynamics and continuous precipitation. Three sites (L1,



L2, and L3; Slesak et al., 2014) were instrumented in 2011 and seven in June 2016 following the same protocols. At each site, we placed a fully-slotted observation well (schedule 40 PVC, 2-inch diameter, 0.010-inch-wide slots) at approximately the lowest elevation; at the flatter L sites, wells were placed at the approximate geographic center of each site. We instrumented each well with a high-resolution total pressure transducer (HOBO U20L-04, resolution = 0.14 cm, average error = 0.4 cm) to record water level time series at 15-minute intervals. We dug each well with a hand auger to a depth associated with the local clay mineral layer and did not penetrate the mineral layer, which ranged from 30 cm below the soil surface to depths greater than 200 cm. We then backfilled each well with a clean, fine sand (20-40 grade). At each site, we also placed a dry well with the same pressure transducer model to measure temperature-buffered barometric pressure and frequency for barometric pressure compensation (McLaughlin and Cohen 2011).

2.4 Data analysis

2.4.1 Hydrology

We calculated simple hydrologic metrics based on the three years of water table data for each site. For each site, we calculated the mean and variance of water table elevation relative to ground surface at the well. A positive water table value indicates that the water table is above the soil surface (inundated conditions), and a negative water table indicates that the water table is below the soil surface. We also calculated the average hydroperiod of each site by counting the number of days that the mean daily water table was above the soil surface at the well each year, and averaging across years.

2.4.2 Elevation distributions

Our first line of inquiry was to evaluate the general spatial distribution of elevation at each site. We first calculated site-level omni-directional and directional (0° , 45° , 90° , 135°) semivariograms using the *gstat* package in R (Pebesma 2004 and Gräler 2016). We calculated directional variograms to test for effects of anisotropy (directional dependence) of elevation. Semivariogram analysis is regularly used in spatial ecology to determine spatial correlation between measurements (Ettema and Wardle 2002). The sill, which is the horizontal asymptote of the semivariogram, is approximately the total variance in parameter measurements. The nugget is the semivariogram y-intercept, and it represents the parameter variance due to sampling error or the inability of sampling resolution to capture parameter variance at small scales. The larger the difference between the sill and the nugget (the “partial sill”), the more spatially predictable the parameter. If the semivariogram is entirely represented by the nugget (i.e., slope = 0), the parameter is randomly spatially distributed. The semivariogram range is the distance where the semivariogram reaches its sill, and it represents the spatial extent (patch size) of heterogeneity, beyond which data are randomly distributed. When spatial dependence is present, semivariance will be low at short distances, increase for intermediate distances, and reach its sill when data are separated by large distances. We used detrended elevation models for this analysis to assess more directly the importance of microtopography on elevation variation as opposed to having it obscured by site-level elevation gradients. From these semivariograms we calculated the best-fit semivariogram model among exponential, Matérn, or Matérn with Stein parameterization model forms (Minasny and McBratney 2005). We also extracted semivariogram nuggets, ranges, sills, and partial sills.



Our second line of inquiry was to evaluate the degree of elevation bimodality in these systems, which is indicative of a positive feedback between hummock growth and hummock height (Eppinga et al., 2008). Based on the classification into hummock or hollow from our delineation algorithm, we plotted site-level detrended elevation distributions for hummocks and hollows and determined a best-fit Gaussian mixture model with Bayesian Information Criteria (BIC) using the *mclust* package (Scrucca et al., 2016) in R (R Core Team 2018), which uses an expectation-maximization algorithm. Mixture models were allowed to have either equal or unequal variance, and were constrained to a comparison of bimodal versus a unimodal mixture distribution.

2.4.3 Subsurface topographic control on microtopography

We assessed the importance of mineral layer microtopography on soil surface microtopography by comparing the depth-to-mineral-layer measurements with the soil surface elevation TLS measurements. We first calculated the elevation of the mineral layer relative to each site-level datum by subtracting the depth-to-mineral-layer measurement from its co-located soil elevation measurement estimated from the TLS campaign. We then plotted the depth-to-mineral-layer measurement (hereafter referred to as “organic soil thickness”) as a function of this mineral layer elevation, noting which points were on hummocks or hollows as determined from the TLS delineation algorithm. We fit linear models to these points and compared the regression slopes to the expected slopes from: 1) a scenario where surface microtopography is simply a reflection of subsurface microtopography (slope = 0, or constant organic soil thickness), and 2) a scenario of flat soil surface where organic soil thickness negatively corresponds to varying mineral layer elevation (slope = -1, or varying soil thickness). Again, the first observation would suggest that surface microtopography mimics subsurface microtopography, whereas the second would suggest organic matter/surface soil accumulation and smoothing over a varying subsurface topography. Observations above the -1:1 line would indicate surface processes that increase elevation above expectations for a flat surface.

2.4.4 Hydrologic controls on microtopography

To test our hypothesis that hydrology is a broad, site-level control on hummock height, we first regressed site mean hummock height against site mean daily water table. We also conducted a within-site regression of individual hummock heights against their local mean daily water table. To do so we first calculated a local relative mean water table for each delineated hummock location by subtracting the elevation minimum of the hummock (i.e., the elevation at the base of the hummock) from the site-level mean water table. This calculation assumes that the water table is flat across the site, which is likely valid for the high permeability organic soils at each site and relatively small areas that we assessed. This within-site regression allowed us to understand more local-scale controls on hummock height.

2.4.5 Hummock spatial distributions

To test whether there was regular spatial patterning of hummocks at each site, we compared the observed distribution of hummocks against a theoretical distribution of hummocks subject to complete spatial randomness (CSR) with the R package *spatstat* (Baddeley et al., 2015). We first extracted the centroids and areas of the hummocks using TopoSeg and created a marked point pattern of the data. Using this point pattern, we conducted a nearest-neighbor analysis



(Diggle 2002), which evaluates the degree of dispersion in a spatial point process (i.e., how far apart on average hummocks are from each other). If hummocks are on average further apart (using the mean nearest neighbor distance, μ_{NN}) compared to what would be expected under CSR (μ_{exp}), the hummocks are said to be overdispersed and subject to regular spacing; if hummocks are closer together than what CSR predicts, they are said to be underdispersed and subject to clustering. We compared the ratio of μ_{NN} and μ_{exp} , where values greater than 1 indicate overdispersion and values below 1 indicate clustering, and calculated a z-score (z_{ANN}) and subsequent p-value to evaluate the significance of overdispersion or clustering (Diggle 2002, Watts et al., 2014). We computed the z-score from the difference between μ_{NN} and μ_{exp} scaled by the standard error. We also evaluated the probability distribution of observed nearest neighbor distances to visualize further the dispersion of wetlands in the landscape.

405 2.4.6 Hummock size distributions

To test the prediction that hummock sizes are constrained by patch-scale negative feedbacks, we plotted site-level rank-frequency curves (inverse cumulative distribution functions) for hummock perimeter, area, and volume. These curves trace the cumulative probability of a hummock dimension (perimeter, area, or volume) being greater than or equal to a certain value ($P[X \geq x]$). We then compared best-fit power ($P[X \geq x] = \alpha X^\beta$), log-normal ($P[X \geq x] = \beta \ln(X) + \beta_0$), and exponential ($P[X \geq x] = \alpha e^{-\beta X}$) distributions for these curves using AIC values. Power-scaling of these curves occurs where negative feedbacks to hummock size are controlled at the landscape-scale (i.e., hummocks have equal probability to be found at all size classes). Truncated scaling of these curves, as in the case of exponential or lognormal distributions, occurs when negative feedbacks to hummock size are controlled at the patch-scale (Scanlon et al., 2007, Watts et al., 2014).

415 3 Results

3.1 Hydrology

Hydrology varied across sites, but largely corresponded to hydrogeomorphic categories (Table 2). Depressions sites were the wettest sites (mean daily water table = -0.010 m), followed by transition sites (-0.039 m), and lowland sites (-0.324 m). Lowland sites also exhibited significantly more variability in water table than transition or depression sites, whose water tables were consistently within 0.4 m of the soil surface. Although lowland sites exhibited greater water table drawdown during the growing season, they were able to rapidly re-wet after rain events.

3.2 Elevation distributions

During field sampling, we observed distinct differences in microtopography among site categories. Depression sites were dominated by hollow features that were punctuated with hummocks associated with black ash trees. Transition sites were microtopographically similar to depression sites, but tended to have more of their area covered with hummocks. Transition site hummocks were also more regularly occupied by canopy species other than black ash, most commonly northern white-cedar, and hummocks were often covered entirely by moss species, especially *Sphagnum spp.* Lowland sites had considerably less variability in microtopography than depression or transition sites,



430 and during the summer were covered in grasses and sedges that obscured hummock and hollow features. However,
during late autumn, it became clear that there were some distinctive hummock features associated with black ash trees,
but these hummocks were far less numerous and less pronounced than those at depression or transition sites. Most
areas of these lowland sites were of intermediate elevation, belonging neither to what would be traditionally considered
hummock nor hollow categories.

435 In support of our observations, semivariograms demonstrated much more pronounced elevation variability at
depression and transition sites than at lowland sites (Figure 4). In general, lowland sites reached overall site elevation
variance (sills, horizontal dashed lines) within 5 meters, but best-fit ranges (dotted vertical lines in Figure 4) were less
than 1 m. In contrast, best-fit semivariogram ranges for depression and transition sites were several times greater.
Therefore, depression and transition sites have much larger ranges of spatial autocorrelation for elevation than
lowland sites. Semivariograms were all best fit with Matérn models with Stein parameterizations, and nugget effects
440 were extremely small in all cases (average <0.001), which we attribute to the very high precision of the TLS method.
As such, partial sills were quite large (i.e., the difference between the sill and nugget), indicating that very little
elevation variation is at scales less than our surface model resolution (1 cm); the remaining variation is found over
site-level ranges of autocorrelation. We did not observe major differences in directional semivariograms compared to
the omnidirectional semivariogram, implying isotropic variability in elevation, and do not present them here

445 We observed bimodal elevation distributions at every site, with hummocks clearly belonging to a distinct elevation
class separate from hollows (Figure 5). Bimodal mixture models of two normal distributions were always better fit to
the data than unimodal models based on BIC values. Differences in mean elevations between these two classes ranged
from 12 cm at the lowland sites to 20 cm at depression sites, and hummock elevations were more variable than hollow
elevations across sites. Across sites, $27\pm 10\%$ of all elevations did not fall into either a hummock or a hollow category,
450 with lowland sites having considerably more elevations failing to fall into these binary categories (36–44%) than
depression (22–27%) or transition sites (16–22%). However, we emphasize that even when considering the entire site
elevation distribution (i.e., including elevations that did not fall into a hummock or hollow category), bimodal fits
were still better than unimodal fits, but to a lesser extent for lowland sites (Figure S3). Delineated hummocks varied
in number and size across and within sites. We observed the greatest number of hummocks in the depression and
455 transition sites, with approximately an order of magnitude less hummocks found in lowland sites (Figure 5).

3.3 Subsurface topographic control on microtopography

Across sites, depth to resistance (“organic soil thickness”) varied and was greatest at the lowest mineral layer
elevations, indicating that surface microtopography is not simply a reflection of subsurface mineral layer topography
with constant overlying organic thickness (as illustrated with 0-slope line in Figure 6). In contrast, at most sites, except
460 for possibly D1 and L2, there was a strong negative linear relationship between soil thickness and mineral layer
elevation, with five sites exhibiting slopes near -1, which we define as the smooth surface model of soil elevation
(dashed -1:1 line in Figure 6). If only hollows (open circles; Figure 6) were used in the regression, then D1 also
exhibited a significant ($p<0.001$) negative slope in this relationship (-0.4 , $R^2 = 0.52$). A majority of depth to mineral
layer measurements at D3 were below detection limit with our 1.5 m steel rod, and all but one measurement at T1



465 were below detection limit. At sites D2 and L2, there was indication that some hollows were actually better represented by the subsurface reflection model (i.e., slope = 0). However, at all sites, though to a lesser extent at lowland sites, hummocks (closed circles; Figure 6) tend to plot above hollows and above the -1:1 line, even when at the same soil thickness as hollows, indicating that their elevation is greater than would be expected for a smooth surface model.

3.4 Hydrologic control on microtopography

470 We observed a significant ($p < 0.001$) positive linear relationship between site level mean hummock height and site level mean daily water table (Figure). Because lowland sites were clearly influential points on this linear relationship, we also conducted this regression excluding the lowland sites and still found a significant ($p = 0.007$) positive linear trend between these variables with reasonable predictive power ($R^2 = 0.8$) — wetter sites have on average have taller hummocks than drier sites. We found very little variability in average hummock heights across sites when relative to
475 site-level mean water table elevation (mean normalized hummock height = 0.31 ± 0.06 m), indicating that hummocks were generally about 30 cm higher than the site mean water table.

Within sites, we also observed clear positive relationships between individual hummock heights and their local mean daily water table (Figure 7). At all but two of the sites (D4 and L1), individual hummock heights within a site were significantly ($p < 0.01$) taller at wetter locations than drier locations. Slopes for these individual hummock regressions
480 varied among sites, ranging from 0.4–1.1 (mean \pm sd = 0.7 ± 0.2), and local hummock mean water table was able to explain 12–56% (mean \pm sd = 0.36 ± 0.14) of variability in hummock height within a site.

3.5 Hummock spatial distributions

All sites characterized as depressions or transitions exhibited significant ($p < 0.001$) overdispersion of hummocks compared to what would be predicted under complete spatial randomness (Figure 8). For these sites, the nearest
485 neighbor ratios ($\mu_{NN}; \mu_{exp}$) indicated that hummocks are 25–30% further apart than would be expected with complete spatial randomness, with spacing ca. 1.5 meters, as evidenced by the narrow distributions in nearest neighbor histograms (Figure). In contrast, all lowland sites, while having hummock nearest neighbor distances 2–3 times as far apart as depression or transition sites, were not significantly different than what would predicted under complete spatial randomness ($p = 0.129, 0.125, 0.04$ for sites L1, L2, and L3, respectively).

490 3.6 Hummock size distributions

Hummock dimensions (perimeter, area, and volume) were strongly lognormally distributed across sites (Figure 9), though exponential models were typically only slightly worse fits. For each hummock dimension, site fits were similar within site hydrogeomorphic categories, but drier lowland site distributions were clearly different from wetter depression and transition site distributions, which were more similar (Figure 9). Lowland sites had significantly lower
495 ($p < 0.05$) coefficients for hummock property model fits than depression or transition sites, with slopes approximately 20% more negative on average, indicating more rapid truncation of size distributions. Across sites, average hummock perimeter was 4.2 ± 0.8 m, average hummock area was 1.7 ± 0.5 m², and average hummock volume was 0.17 ± 0.06 m³. Hummock areas were typically less than 1 m² in size at all sites (Figure 9). Similar to hummock spatial density,



500 hummock area per site (ratio of hummock area to site area) was lower at drier lowland sites (2–5%) compared to wetter depression and transition sites (12–22%) (Figure 5).

4 Discussion

We tested our hypothesis that microtopography in black ash wetlands self-organizes in response to hydrologic drivers (Figure 1) using an array of diagnostic tests including analyses of multimodal elevation distributions, spatial patterning, and patch size distributions. We further analyzed the influence of hydrology on these diagnostic measures
505 and tested a potential null hypothesis that surface microtopography was simply a reflection of subsurface microtopography. Diagnostic test results and clear hydrologic influence on microtopographic structure provide strong support for our hypothesis.

4.1 Controls on microtopographic structure

Bimodal soil elevation distributions at all sites suggest that the microsite separation into hummocks and hollows is a
510 common attribute of black ash wetlands. Soil elevation bimodality was most evident at depression and transition sites, where hummocks were more numerous and occupied a higher fraction of overall site area (15–20%). Sharp boundaries between hummocks and hollows were not always observed in soil elevation probability densities (Figure 5), which may be indicative of weaker-than-predicted positive feedbacks between primary productivity and elevation (Rietkerk et al., 2004; Figure 1). On the other hand, modeling predictions indicate that if evapoconcentration feedbacks are strong, boundaries between hummocks and hollows will be less sharp (Eppinga et al., 2009), possibly implicating
515 hummock evapoconcentration as an additional feedback to hummock maintenance (Figure 1).

Our results provide clear evidence of decoupling between surface microtopography and mineral layer microtopography at all of our sites. A smooth surface model, with a relatively constant surface elevation despite variable underlying mineral soil elevation, best represented hollows. Importantly, we also observed that regardless of
520 underlying mineral layer, hummocks had greater soil thickness than hollows did (Figure). To clarify, irrespective of mineral layer microtopography, hummocks are maintained at local elevations that are higher than would be predicted for a smooth soil surface. We interpret this as evidence for self-organization of wetland microtopography. Smoothing of soil surfaces relative to variability in underlying mineral layers or bedrock is observed in other wetland systems where soil creation is dominated by organic matter accumulation (Watts et al., 2014), implying that deviations from
525 this smooth surface are related to other surface-level processes.

Hummock heights relative to site-level water table were approximately 30 cm, aligning with field observations of relatively constant hummock height within sites. Generally consistent hummock height across sites in conjunction with clear bimodality in soil elevations supports the contention that hummocks and hollows are discrete, self-organized ecosystem states (*sensu* Watts et al., 2010). However, variability in site-level hummock heights—especially at
530 depression and transition sites—may partially be attributable to hummocks in non-equilibrium states. From our feedback model (Figure 1), it seems reasonable that within a site, some hummocks may be in growing states (e.g., elevation-GPP positive feedback) and some may be in shrinking states (e.g., elevation-respiration negative feedback),



the combination of which may result in a distribution of hummock heights centered around an equilibrium hummock height.

535 We observed strong control of local hydrology on hummock height, providing evidence for our hypothesis that hummocks are a biogeomorphic response to hydrologic stresses in wetlands. Vegetation patches like hummocks are most commonly found in conditions with strong environmental stressors. In particular, water stress—both too little (Deblauwe et al., 2008, Scanlon et al., 2007) and too much (Eppinga et al., 2009)—appears to be an important regulator of microhabitat size and its spatial distribution across the landscape. Wetlands are characterized by regular water stresses from periodic inundation with nearly all biogeochemical processes under the fundamental influence of hydrology (Rodriguez-Iturbe et al., 2007). It is therefore perhaps unsurprising that hydrology also controls the scale-dependent feedbacks that create and maintain hummock sizes and their spatial patterning. We found support for this contention at both the site level and at the hummock level, with the tallest hummocks being found in the wettest sites and in the wettest zones within sites. In fact, distance from mean water table explained on average 35% of the variability in hummock height (Figure); prevalence of non-equilibrium hummock states may explain much of the additional variability. The considerable variation in the ability of hydrology to explain hummock height within sites (adjusted $R^2 = 0.12\text{--}0.56$), and also in the strength of that relationship (linear regression slopes=0.4–1.1) may be attributed to two factors: 1) the across-site flat water table assumption, and 2) lack of long trends for hydrology. The flat water table assumption is likely to be a minor effect in transition sites with deep organic wetland soils (e.g., Nungesser 2003, Wallis and Raulings 2011, Cobb et al., 2017), but could be significant at depression and lowland sites with shallower O horizons. Lack of sufficient data to characterize mean water table may also be an issue at several of our sites, because hummocks likely develop over the course of decades or more, whereas our hydrology data only span three years.

To our knowledge, this study represents the first empirical evidence of the positive relationship between hummock height and hydrology in forested wetlands. These results are consistent with previous research on tussocks of northern wet meadows (Peach and Zedler 2006, Lawrence and Zedler 2011) and shrub hummocks in brackish wetlands (Wallis and Raulings 2011). The concordance in hydrologic control in these disparate systems suggests a common mechanism of soil building and accumulation on hummocks that may result from increased vegetation growth from reduced water stress and/or from transport and accumulation of nutrients (Eppinga et al., 2009, Sullivan et al., 2011, Heffernan et al., 2013).

4.2 Controls on microtopographic patterning

We found clear support for our hypothesis that hummocks are non-randomly distributed in the wettest sites of our study area, further supporting the posited interactions among hydrology, vegetation, and soils. Hummocks exhibited spatial overdispersion in all sites, but this overdispersion was only significant at depression and transition sites (Figure). Significant spatial overdispersion is indicative of regular hummock spacing in contrast to clustered distributions or completely random placement. Regular patterning of landscape elements is observed across climates, regions, and ecosystems (Rietkerk and van de Koppel 2008), but to our knowledge, this study is the first to demonstrate regular patterning in forested wetland microtopography and the hydrologic control on this regular pattern emergence.



Hydrology appears to be a common driver in regular pattern formation in wetlands (Heffernan et al., 2013), drylands
570 (Scanlon et al., 2007), and tidal flats (Weerman et al., 2011) through a diverse array of mechanisms (e.g., Watts et al.,
2014). However, most observed regular patterning in wetlands ultimately develops only through coupling between
biota and hydrology (Rietkerk and van de Koppel 2008), underscoring the importance of biota in structuring their own
environment.

We observed lognormal hummock size distributions, suggesting that some hummocks may attain very large areas (i.e.,
575 over 10 m²), but the majority of hummocks (~80%) are less than 1 m² (Figure 9). This finding aligns with field
observations, where most hummocks were associated with a single black ash tree, but some hummocks appeared to
have merged over time to create large patches. Truncated patch size distributions are common in other systems as
well, like the stretched exponential distribution for geographically isolated wetlands (Watts et al., 2014) or the
lognormal distribution for desert soil crusts (Bowker et al., 2013). These types of distributions have much fewer large
580 patches than would be expected for systems without patch-scale negative feedbacks, and have a central tendency
towards a common patch size. Hence, truncation in hummock size distributions comports with hypothesized patch-
scale negative feedbacks (i.e., tree competition for light and nutrients) that inhibit expansion. Hummocks at drier
lowland sites did not conform to size distributions or spatial patterns from wetter depression and transition sites,
supporting our hypothesis that the feedbacks that control hummock maintenance and distribution are governed by
585 hydrology and amplified in wetter conditions. Larger hummock patches were especially obvious at transition sites that
had significant *Sphagnum spp.* moss cover, which tended to blend and expand hummock areas. This work adds to
recent efforts across climates and systems to use patch size distributions to infer drivers and processes of ecosystem
self-organization and response to environmental conditions and abiotic drivers (Kefi et al., 2007, Maestre and
Escudero 2009, Weerman et al., 2011, Schoelynck et al., 2012, Tamarelli et al., 2017).

Characteristic hummock sizes in association with overdispersion in black ash wetlands suggest that hummocks are
590 laterally limited in size by negative feedbacks on the scale of meters (Manor and Shnerb 2008). We posit that there
are two patch-scale negative feedbacks: 1) overstory competition for nutrients and 2) understory and overstory
competition for light. Hummocks associated with black ash trees, which account for more than 85% of measured
hummocks, are likely limited in area by the radial growth of the tree's root system. Evapoconcentration feedbacks
595 bring nutrients to the tree roots, limiting the degree to which roots must search for them (Karban 2008), and therefore
limiting root lateral expansion. Moreover, finite nutrient pools may lead to development of similarly sized nutrient
source basins for each hummock, further limiting expansion (Rietkerk et al., 2004, Eppinga et al., 2008). Black ash
trees must also compete for light with other ash trees, but leaf area is typically low in these systems (<2.5 leaf area
index [LAI]; Telander et al., 2015). Low LAI and observed canopy shyness (*sensu* Long and Smith 1992) in black ash
600 wetlands may imply less competition among individuals than would be expected in mixed stands (Franco 1986). On
the other hand, low canopy competition for light in the overstory may increase light availability for understory
hummock species, and therefore allow subsequent hummock expansion from the understory.



4.3 Broader implications

The consequences of wetland microtopography are clear at small scales, but there is also some evidence that the presence of microtopography has site- and regional-scale importance. For example, microtopographic expression results in a drastic increase in surface area within wetlands. We estimate an average of 19% and up to 32% relative increase in surface area due to the presence of hummocks (i.e., that additional area provided by the sides of hummocks; Table 23). These estimates comport with studies in tussock meadows that found tussocks of an average of 20 cm tall increased surface area by up to 40% (Peach and Zedler 2006). Increases in the diversity of biogeochemical processes occurring at the individual hummock or hollow scale (Deng et al., 2014) likely aggregate to influence ecosystem functioning at large scales. For example, microtopographic niche expansion allows for local material and solute exchange between hummocks and hollows, creating coupled aerobic-anaerobic conditions with emergent outcomes for denitrification (Frei et al., 2012) and carbon emission (Bubier et al., 1995).

While our results implicate hydrology as a major determinant of microtopographic structure and pattern, microtopography can reciprocally influence system-scale hydraulic properties. Results from our hummock property analysis indicate that hummock volume displacement may be a significant factor in water table dynamics of wetlands. Specific yield, which controls water table response to hydrologic fluxes, is commonly assumed to be unity when wetlands are inundated. However, inclusion of microtopography may render this assumption invalid, with hummock volumes up to 30% of site volumes (Table 4). These observations are supported in other studies of microtopographic effects of specific yield (Sumner 2007, McLaughlin and Cohen 2014, Dettmann and Bechtold 2016). Therefore, while hydrology exerts clear control on the geometry of hummocks, hummocks may exert reciprocal control on hydrology by amplifying small hydrologic fluxes into large water table variations

Last, hummocks also provide unique microsite conditions that support increased vegetation growth and diversity (Bledsoe and Shear 2000, Peach and Zedler 2006, Økland et al., 2008). Evidence abounds for both increased understory richness and improved seedling regeneration on hummocks relative to hollows (Koponen et al., 2004, Dubertstein and Connor 2009, Courtwright and Findlay 2011). To this point, recent wetland restoration efforts have begun to use microtopography as a restoration strategy to promote planted seedling success and long-term project viability (Larkin et al., 2006; Bannister et al., 2013; Liefers et al., 2017). Indeed, and in light of recent concerns over regime shift to marsh like states from black ash loss to EAB (Diamond et al., 2018), we posit that hummock presence and persistence may allow for future tree seedlings to survive wetting up periods following ash loss (Slesak et al., 2014), and for consequent resilience of swamp ecosystem states.

5 Conclusions

Although observations of the presence and significance of wetland microtopography abound in the literature, this is the first study, to our knowledge, to detail the structure, pattern, and drivers of wetland microtopography in forested systems. This study adds to the growing body of evidence that the structure and regular patterning of wetland microtopography is an autogenic response to hydrology. Although the imprint of biota on landscapes may be masked



by the signature of larger scale physical processes (Dietrich and Perron, 2006), we show clear evidence here for a microtopographic signature of life.

6 Code and data availability

640 The authors will provide code and data upon request, and will upload code to Github upon acceptance of the manuscript.

7 Author contribution

JD and DM created the conceptual framework, questions, and hypotheses. AS and JD developed the TLS procedure and carried out measurements and subsequent analysis/code; JD and RS carried out hydrology measurements. JD
645 conducted all data analysis and wrote the manuscript. All co-authors contributed significantly to editing the manuscript.

8 Competing interests

The authors declare that they have no conflict of interest.

9 Acknowledgments

650 This project was funded by the Minnesota Environmental and Natural Resources Trust Fund, the USDA Forest Service Northern Research Station, and the Minnesota Forest Resources Council. Additional funding was provided by the Virginia Tech Forest Resources and Environmental Conservation department, the Virginia Tech Institute for Critical Technology and Applied Science, and the Virginia Tech William J. Dann Fellowship. We gratefully acknowledge the field work and data collection assistance provided by Mitch Slater, Alan Toczydlowski, and Hannah Friesen.

655 10 References

- Amundson, R., Richter, D. D., Humphreys, G. S., Jobbágy, E. G., and Gaillardet, J.: Coupling between biota and earth materials in the critical zone, *Elements*, 3(5), 327–332, 2007.
- Baddeley A., Rubak, E., and Turner, R.: *Spatial Point Patterns: Methodology and Applications with R*. London: Chapman and Hall/CRC Press, 2015, URL <http://www.crcpress.com/Spatial-Point-Patterns-Methodology-and-Applications-with-R/Baddeley-Rubak-Turner/9781482210200/>, 2015.
- 660 Bannister, J. R., Coopman, R. E., Donoso, P. J., and Bauhus, J.: The Importance of Microtopography and Nurse Canopy for Successful Restoration Planting of the Slow-Growing Conifer *Pilgerodendron uviferum*, *Forests* 4:85–103, 2013.
- Belyea, L. R., and Baird, A. J.: Beyond “the limits to peat bog growth”, Cross-scale feedback in peatland development. *Ecological Monographs*, 76(3), 299–322, 2006.
- 665



- Bledsoe, B. P. and Shear, T. H.: Vegetation along hydrologic and edaphic gradients in a North Carolina coastal plain creek bottom and implications for restoration, *Wetlands*, 20:126–147, 2000.
- Bowker, M. A., Maestre, F. T., and Mau, R. L.: Diversity and patch–size distributions of biological soil crusts regulate dryland ecosystem multifunctionality, *Ecosystems*, 16(6), 923–933, 2013
- 670 Brantley, S. L., Eissenstat, D. M., Marshall, J. A., Godsey, S. E., Balogh-Brunstad, Z., Karwan, D. L., and Chadwick, O.: Reviews and syntheses: on the roles trees play in building and plumbing the critical zone, *Biogeosciences (Online)*, 14(22), 2017.
- Bubier, J. L., Moore, T. R., Bellisario, L., Comer, N. T., and Crill, P. M.: Ecological controls on methane emissions from a northern peatland complex in the zone of discontinuous permafrost, Manitoba, Canada, *Global Biogeochemical Cycles*, 9(4), 455–470, 1995.
- 675 Cobb, A. R., Hoyt, A. M., Gandois, L., Eri, J., Dommain, R., Salim, K. A., and Harvey, C. F.: How temporal patterns in rainfall determine the geomorphology and carbon fluxes of tropical peatlands, *Proceedings of the National Academy of Sciences*, 114(26), E5187–E5196, 2017.
- Conner, W. H.: Woody plant regeneration in three South Carolina *Taxodium/Nyssa* stands following Hurricane Hugo, *Ecological Engineering* 4:227–287, 1995.
- 680 Corenblit, D., Baas, A. C., Bornette, G., Darrozes, J., Delmotte, S., Francis, R. A., and Steiger, J.: Feedbacks between geomorphology and biota controlling Earth surface processes and landforms: a review of foundation concepts and current understandings, *Earth–Science Reviews*, 106(3–4), 307–331, 2011.
- Courtwright, J. and Findlay, S. E., Effects of microtopography on hydrology, physicochemistry, and vegetation in a tidal swamp of the Hudson River, *Wetlands*, 31(2), 239–249, 2011.
- 685 D’Amato, A., Palik, B., Slesak, R., Edge, G., Matula, C., and Bronson, D.: Evaluating Adaptive Management Options for Black Ash Forests in the Face of Emerald Ash Borer Invasion, *Forests*, 9(6), 348, 2018.
- Deblauwe, V., Barbier, N., Couteron, P., Lejeune, O., and Bogaert, J.: The global biogeography of semi-arid periodic vegetation patterns, *Global Ecology and Biogeography*, 17(6), 715–723, 2008.
- 690 Deng, Y., Cui, X., Hernández, M., and Dumont, M. G.: Microbial Diversity in Hummock and Hollow Soils of Three Wetlands on the Qinghai–Tibetan Plateau Revealed by 16S rRNA Pyrosequencing, *PLOS ONE* 9:e103115, 2014.
- Dettmann, U., and Bechtold, M.: One-dimensional expression to calculate specific yield for shallow groundwater systems with microrelief, *Hydrological Processes*, 30(2), 334–340, 2016.
- Dietrich, W. E., and Perron, J. T.: The search for a topographic signature of life, *Nature*, 439(7075), 411, 2006.
- 695 Diggle, P.J.: *Statistical Analysis of Spatial Point Patterns*, 2nd edn. Hodder Education: London; 288, 2002.
- Duberstein, J. A., Krauss, K. W., Conner, W. H., Bridges Jr., W. C., and Shelburne, V.B.: Do Hummocks Provide a Physiological Advantage to Even the Most Flood Tolerant of Tidal Freshwater Trees?, *Wetlands* 33: 399–408, 2013.
- Eppinga, M. B., De Ruyter, P. C., Wassen, M. J., and Rietkerk, M.: Nutrients and hydrology indicate the driving mechanisms of peatland surface patterning, *The American Naturalist*, 173(6), 803–818, 2009.
- 700 Erdmann, G. G., Crow, T. R., Ralph Jr, M., and Wilson, C. D.: Managing black ash in the Lake States. General Technical Report NC–115. St. Paul, MN: US Dept. of Agriculture, Forest Service, North Central Forest Experiment Station, 115, 1987.



- Ettema, C. H. and Wardle, D. A.: Spatial soil ecology, *Trends in ecology and evolution*, 17(4), 177–183, 2002.
- 705 Foti, R., del Jesus, M., Rinaldo, A., and Rodriguez-Iturbe, I.: Hydroperiod regime controls the organization of plant species in wetlands, *Proceedings of the National Academy of Sciences*, 109(48), 19596–19600, 2012.
- Franco, M.: The influence of neighbours on the growth of modular organisms with an example from trees, *Philosophical Transactions of the Royal Society of London. B, Biological Sciences*, 313(1159), 209–225, 1986.
- Frei, S., Knorr, K. H., Peiffer, S., and Fleckenstein, J. H.: Surface micro-topography causes hot spots of biogeochemical activity in wetland systems: A virtual modeling experiment, *Journal of Geophysical Research: Biogeosciences*, 117(G4), 2012.
- 710 Gabet, E. J., Perron, J. T., and Johnson, D. L.: Biotic origin for Mima mounds supported by numerical modelling, *Geomorphology*, 206, 58–66, 2014.
- Gräler, B., Pebesma, E., and Heuvelink, G.: Spatio-Temporal Interpolation using gstat, *The R Journal* 8(1), 204–218, 2016.
- 715 Heffernan, J. B., Watts, D. L., and Cohen, M. J.: Discharge competence and pattern formation in peatlands: a meta-ecosystem model of the Everglades ridge-slough landscape, *PloS one*, 8(5), e64174, 2013.
- Huenneke, L. F., and Sharitz, R. R.: Substrate heterogeneity and regeneration of a swamp tree, *Nyssa aquatic*, *American Journal of Botany*, 77(3), 413–419, 1990.
- Jackson, R. B., and Caldwell, M. M.: Integrating resource heterogeneity and plant plasticity: modelling nitrate and phosphate uptake in a patchy soil environment, *Journal of Ecology*, 891–903, 1996.
- 720 Karban, R.: Plant behaviour and communication. *Ecology letters*, 11(7), 727–739, 2008.
- Kéfi, S., Rietkerk, M., Alados, C. L., Pueyo, Y., Papanastasis, V. P., ElAich, A., and De Ruiter, P. C.: Spatial vegetation patterns and imminent desertification in Mediterranean arid ecosystems, *Nature*, 449(7159), 213, 2007.
- Kéfi, S., Rietkerk, M., Roy, M., Franc, A., De Ruiter, P. C., and Pascual, M.: Robust scaling in ecosystems and the meltdown of patch size distributions before extinction, *Ecology letters*, 14(1), 29–35, 2011.
- 725 Koponen, P., Nygren, P., Sabatier, D., Rousteau, A., and Saur, E.: Tree species diversity and forest structure in relation to microtopography in a tropical freshwater swamp forest in French Guiana, *Plant Ecology*, 173(1), 17–32, 2004.
- Kurmis, V., and Kim, J. H.: Black ash stand composition and structure in Carlton County, Minnesota, 1989.
- Larkin, D. J., Vivian-Smith, G., and Zedler, J.B.: Topographic heterogeneity theory and ecological restoration. In: Falk, D. A., Palmer, M.A., and Zedler, J.B., (eds), *Foundations of restoration ecology*. Island Press, Washington, D.C., USA, 2006.
- 730 Larsen, L. G., and Harvey, J. W.: Modeling of hydroecological feedbacks predicts distinct classes of landscape pattern, process, and restoration potential in shallow aquatic ecosystems, *Geomorphology*, 126(3–4), 279–296, 2011.
- Lashermes, B., Foufoula-Georgiou, E., and Dietrich, W. E.: Channel network extraction from high resolution topography using wavelets, *Geophysical Research Letters*, 34(23), 2007.
- 735 Lawrence, B. A., and Zedler, J. B.: Formation of tussocks by sedges: effects of hydroperiod and nutrients, *Ecological Applications*, 21(5), 1745–1759, 2011.
- Lieffers, V. J., Caners, R.T., and Ge, H.: Re-establishment of hummock topography promotes tree regeneration on highly disturbed moderate-rich fens, *Journal of Environmental Management*, 197:258–264, 2017.



- 740 Long, J. N., and Smith, F. W.: Volume increment in *Pinus contorta* var. *latifolia*: the influence of stand development and crown dynamics, *Forest Ecology and Management*, 53(1-4), 53–64, 1992.
- Maestre, F. T., and Escudero, A.: Is the patch size distribution of vegetation a suitable indicator of desertification processes?, *Ecology*, 90(7), 1729–1735, 2009.
- Manor, A., and Shnerb, N. M.: Facilitation, competition, and vegetation patchiness: from scale free distribution to
- 745 patterns, *Journal of theoretical biology*, 253(4), 838–842, 2008.
- McLaughlin, D. L., and Cohen, M. J.: Ecosystem specific yield for estimating evapotranspiration and groundwater exchange from diel surface water variation, *Hydrological Processes*, 28(3), 1495–1506, 2014.
- Minasny, B., and McBratney, A. B.: The Matérn function as a general model for soil variograms, *Geoderma*, 128(3–4), 192–207, 2005.
- 750 Nungesser, M. K.: Modelling microtopography in boreal peatlands: hummocks and hollows, *Ecological Modelling*, 165(2–3), 175–207, 2003.
- Økland, R. H., Rydgren, K., and Økland, T.: Species richness in boreal swamp forests of SE Norway: The role of surface microtopography, *Journal of Vegetation Science*, 19(1), 67–74, 2008.
- Othmani, A., Piboule, A., Krebs, M., Stolz, C., Voon, L.L.Y.: Towards automated and operational forest inventories with T-Lidar, in: 11th International Conference on LiDAR Applications for Assessing Forest Ecosystems (SilviLaser 2011), 2011.
- 755 Pascual, M., Roy, M., Guichard, F., and Flierl, G.: Cluster size distributions: signatures of self-organization in spatial ecologies, *Philosophical Transactions of the Royal Society of London. Series B: Biological Sciences*, 357(1421), 657–666, 2002.
- 760 Pascual, M., and Guichard, F.: Criticality and disturbance in spatial ecological systems, *Trends in ecology and evolution*, 20(2), 88–95, 2005.
- Pau, G., Fuchs, F., Sklyar, O., Boutros, M., Huber, W.: EBImage—an R package for image processing with applications to cellular phenotypes, *Bioinformatics* 26, 979–981. <https://doi.org/10.1093/bioinformatics/btq046>, 2010.
- Pawlik, Ł., Phillips, J. D., and Šamonil, P.: Roots, rock, and regolith: Biomechanical and biochemical weathering by
- 765 trees and its impact on hillslopes—A critical literature review, *Earth–science reviews*, 159, 142–159, 2016.
- Peach, M., and Zedler, J. B.: How tussocks structure sedge meadow vegetation. *Wetlands*, 26(2), 322–335, 2006.
- Pebesma, E.J.: Multivariable geostatistics in S: the gstat package, *Computers and Geosciences*, 30: 683–691, 2004.
- Peterson, J. E., and Baldwin, A.H.: Variation in wetland seed banks across a tidal freshwater landscape, *American Journal of Botany* 91:1251–1259, 2004.
- 770 Planchon, O., Esteves, M., Silvera, N., and Lapetite, J. M.: Microrelief induced by tillage: measurement and modelling of surface storage capacity, *Catena*, 46(2–3), 141–157, 2002.
- Pugnaire, F. I., Haase, P., and Puigdefabregas, J.: Facilitation between higher plant species in a semiarid environment, *Ecology*, 77(5), 1420–1426, 1996.
- R Core Team: R: A language and environment for statistical computing, R Foundation for Statistical Computing, Vienna, Austria, URL <https://www.R-project.org/>, 2018.
- 775



- Reinhardt, L., Jerolmack, D., Cardinale, B. J., Vanacker, V., and Wright, J.: Dynamic interactions of life and its landscape: feedbacks at the interface of geomorphology and ecology, *Earth Surface Processes and Landforms*, 35(1), 78–101, 2010.
- Rietkerk, M., Dekker, S. C., Wassen, M. J., Verkroost, A. W. M., and Bierkens, M. F. P.: A putative mechanism for bog patterning, *The American Naturalist*, 163(5), 699–708, 2004.
- Rietkerk, M., and Van de Koppel, J.: Regular pattern formation in real ecosystems, *Trends in ecology and evolution*, 23(3), 169–175, 2008.
- Roering, J. J., Marshall, J., Booth, A. M., Mort, M., and Jin, Q.: Evidence for biotic controls on topography and soil production, *Earth and Planetary Science Letters*, 298(1–2), 183–190, 2010.
- Roussel, J.R., Auty, D.: *lidR: Airborne LiDAR Data Manipulation and Visualization for Forestry Applications*, 2018.
- Scanlon, T. M., Caylor, K. K., Levin, S. A., and Rodriguez-Iturbe, I.: Positive feedbacks promote power-law clustering of Kalahari vegetation, *Nature*, 449(7159), 209, 2007.
- Scheffer, M., and Carpenter, S. R.: Catastrophic regime shifts in ecosystems: linking theory to observation, *Trends in ecology and evolution*, 18(12), 648–656, 2003.
- Schoelynck, J., De Groot, T., Bal, K., Vandenbruwaene, W., Meire, P., and Temmerman, S.: Self-organised patchiness and scale-dependent bio-geomorphic feedbacks in aquatic river vegetation, *Ecography*, 35(8), 760–768, 2012.
- Schröder, A., Persson, L., and De Roos, A. M.: Direct experimental evidence for alternative stable states: a review, *Oikos*, 110(1), 3–19, 2005.
- Scrucca, L., Fop, M., Murphy, T. B., and Raftery, A. E.: mclust 5: clustering, classification and density estimation using Gaussian finite mixture models, *The R Journal* 8/1, pp. 205–233, 2016.
- Sebestyen, S.D., Dorrance, C., Olson, D.M., Verry, E.S., Kolka, R.K., Elling, A.E., and Kyllander, R.: Chapter 2. Long-term monitoring sites and trends at the Marcell Experimental Forest, In *Peatland biogeochemistry and watershed hydrology at the Marcell Experimental Forest*. Edited by R.K. Kolka, S.D. Sebestyen, E.S. Verry, and K.N. Brooks. Boca Raton, FL: CRC Press: 15–71, 2011.
- Soil Survey Staff, Natural Resources Conservation Service, United States Department of Agriculture. Web Soil Survey. Available online at the following link: <https://websoilsurvey.sc.egov.usda.gov/>. Accessed February 11, 2019.
- Strack, M., Waddington, J. M., Rochefort, L., and Tuittila, E. S.: Response of vegetation and net ecosystem carbon dioxide exchange at different peatland microforms following water table drawdown, *Journal of Geophysical Research: Biogeosciences*, 111(G2), 2006.
- Stribling, J. M., Cornwell, J.C., and Glahn, O.A.: Microtopography in tidal marshes: Ecosystem engineering by vegetation?, *Estuaries and Coasts* 30:1007–1015, 2007.
- Sullivan, P. F., Arens, S.J., Chimner, R.A., and Welker, J.M.: Temperature and microtopography interact to control carbon cycling in a high arctic fen, *Ecosystems*, 11(1), 61–76, 2008.
- Sumner, D. M.: Effects of capillarity and microtopography on wetland specific yield, *Wetlands*, 27(3), 693–701, 2007.
- Taramelli, A., Valentini, E., Cornacchia, L., and Bozzeda, F.: A hybrid power law approach for spatial and temporal pattern analysis of salt marsh evolution, *Journal of Coastal Research*, 77(sp1), 62–72, 2017.



- Telander, A. C., Slesak, R. A., D'Amato, A. W., Palik, B. J., Brooks, K. N., and Lenhart, C. F.: Sap flow of black ash in wetland forests of northern Minnesota, USA: Hydrologic implications of tree mortality due to emerald ash borer, *Agricultural and forest meteorology*, 206, 4–11, 2015.
- 815
- Turner, M. G.: Landscape ecology: what is the state of the science?, *Annu. Rev. Ecol. Evol. Syst.*, 36, 319–344, 2005.
- van de Koppel, J., and Rietkerk, M.: Spatial interactions and resilience in arid ecosystems, *The American Naturalist*, 163(1), 113–121, 2004.
- van De Koppel, J. and Crain, C.M.: Scale-Dependent Inhibition Drives Regular Tussock Spacing in a Freshwater
820 Marsh, *The American Naturalist* 168:E136–E147, 2006.
- von Hardenberg, J., Kletter, A. Y., Yizhaq, H., Nathan, J., and Meron, E.: Periodic versus scale-free patterns in dryland vegetation, *Proceedings of the Royal Society B: Biological Sciences*, 277(1688), 1771–1776, 2010.
- Wallis, E., and Raulings, E.: Relationship between water regime and hummock-building by *Melaleuca ericifolia* and *Phragmites australis* in a brackish wetland, *Aquatic Botany*, 95(3), 182–188, 2011.
- 825 Watts, D. L., Cohen, M. J., Heffernan, J. B., and Osborne, T. Z.: Hydrologic modification and the loss of self-organized patterning in the ridge-slough mosaic of the Everglades, *Ecosystems*, 13(6), 813–827, 2010.
- Watts, A. C., Watts, D. L., Cohen, M. J., Heffernan, J. B., McLaughlin, D. L., Martin, J. B., and Kobziar, L. N.: Evidence of biogeomorphic patterning in a low-relief karst landscape, *Earth Surface Processes and Landforms*, 39(15), 2027–2037, 2014.
- 830 Weerman, E. J., Van Belzen, J., Rietkerk, M., Temmerman, S., Kéfi, S., Herman, P. M. J., and de Koppel, J. V.: Changes in diatom patch-size distribution and degradation in a spatially self-organized intertidal mudflat ecosystem, *Ecology*, 93(3), 608–618, 2012.
- Western Regional Climate Center [WRCC]: Cooperative Climatological Data Summaries, Retrieved from <https://wrcc.dri.edu/cgi-bin/cliMAIN.pl?mn4652>, 2019.
- 835 Wolf, K. L., Ahn, C. and Noe, G.B.: Microtopography enhances nitrogen cycling and removal in created mitigation wetlands, *Ecological Engineering* 37:1398–1406, 2011.



11 Tables

Table 1 Site information for ten black ash study wetlands

Site	Latitude	Longitude	Elevation (m ASL)	Size (ha)	Average organic horizon depth (cm)
D1	47.67168	-93.68438	447	5.697	28.9 ± 9.1
D2	47.28097	-94.38353	425	6.499	27.7 ± 11.3
D3	47.28380	-94.37992	429	6.062	105.3 ± 32.2
D4	47.28021	-94.48627	442	0.491	60.6 ± 22.1
L1	47.53685	-94.21786	403	2.191	28.8 ± 9.5
L2	47.53444	-94.21320	391	6.845	19.6 ± 7.2
L3	47.52744	-94.20573	394	1.455	24.5 ± 10.1
T1	47.83737	-93.71288	424	15.659	129.4 ± 3.6
T2	47.67887	-93.91441	447	8.618	84 ± 26.2
T3	47.27623	-94.48689	432	1.938	53.6 ± 28.5

840



Table 2 Daily water table summary statistics for black ash study wetlands

Site	Mean (m)	Median (m)	Standard deviation (m)	Mean hydroperiod (d)
D1	0.012	0.088	0.179	105
D2	-0.098	0.042	0.156	96
D3	0.053	0.143	0.196	117
D4	-0.008	0.003	0.151	77
L1	-0.255	-0.046	0.462	67
L2	-0.346	-0.046	0.543	77
L3	-0.370	-0.076	0.502	61
T1	-0.001	0.034	0.125	105
T2	-0.048	0.044	0.202	101
T3	-0.069	0.016	0.217	84



Table 3 Relative area increase by hummocks across sites

Site	Survey area (m²)	Hummock side surface area (m²)	Relative area increase by hummocks
D1	1234	175	0.17
D2	919	151	0.14
D3	1221	223	0.20
D4	1045	107	0.09
L1	1041	55	0.04
L2	1093	40	0.04
L3	1164	41	0.03
T1	731	237	0.32
T2	994	227	0.23
T3	1198	179	0.15
Average		144±74	0.14±0.09
(Average, no L)		(186±44)	(0.19±0.07)

845



Table 4 Hummock volume displacement ratios for all sites

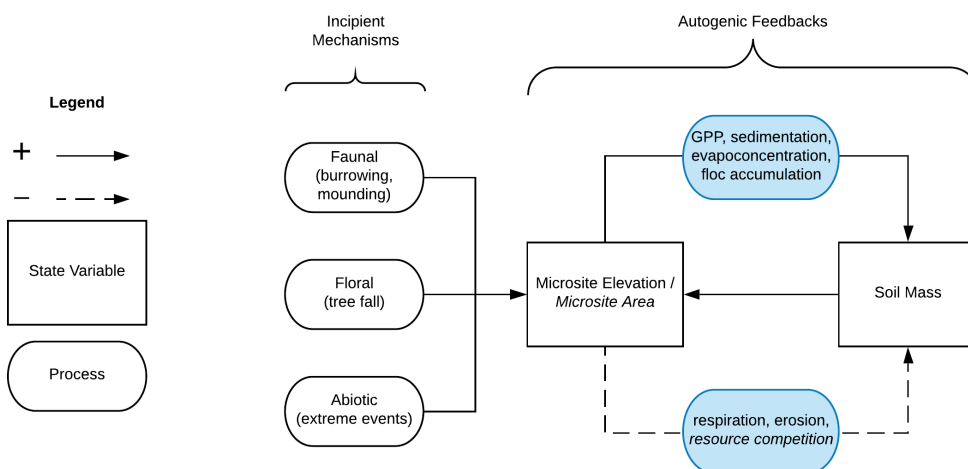
Site	Site height [†] (m)	Site volume [‡] (m ³)	Hummock volume (m ³)	Hummock volume displacement ratio
D1	0.17	179	33	0.18
D2	0.15	155	26	0.17
D3	0.21	233	41	0.18
D4	0.17	200	24	0.12
L1	0.15	181	10	0.05
L2	0.26	242	5	0.02
L3	0.21	255	6	0.02
T1	0.18	134	37	0.28
T2	0.16	157	46	0.30
T3	0.17	199	37	0.18
Average			27±14	0.15±0.09
(Average, no L)			(35±7)	(0.20±0.06)

[†]Site height is estimated as the mean 80th percentile of hummock heights across the site

[‡]Site volume is estimated as by multiplying site height by site area

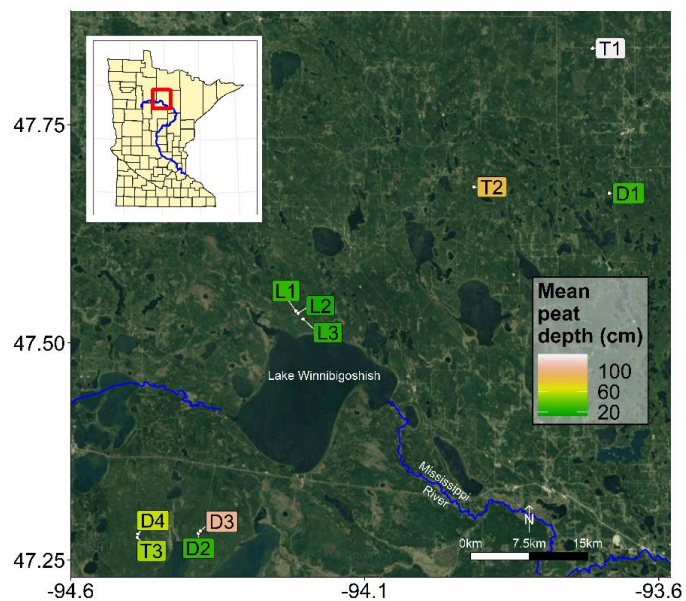


850 12 Figures



855

Figure 1. Conceptual model for autogenic hummock maintenance in wetlands. Incipient mechanisms create small-scale variation in soil elevation that is amplified by autogenic feedbacks, which grow and maintain elevated hummock structures. Solid lines indicate positive feedback loops and dashed lines indicate negative feedback loops. Font in *italics* refer to feedback processes hypothesized to only affect lateral hummock extent (thus hummock area), whereas non-*italic* font indicates mechanisms that affect both vertical and lateral hummock extent. Processes in blue indicate that these mechanisms are influenced by hydrology.



860 Figure 2. Map of black ash wetland sites. Sites are colored by their mean organic horizon depth.

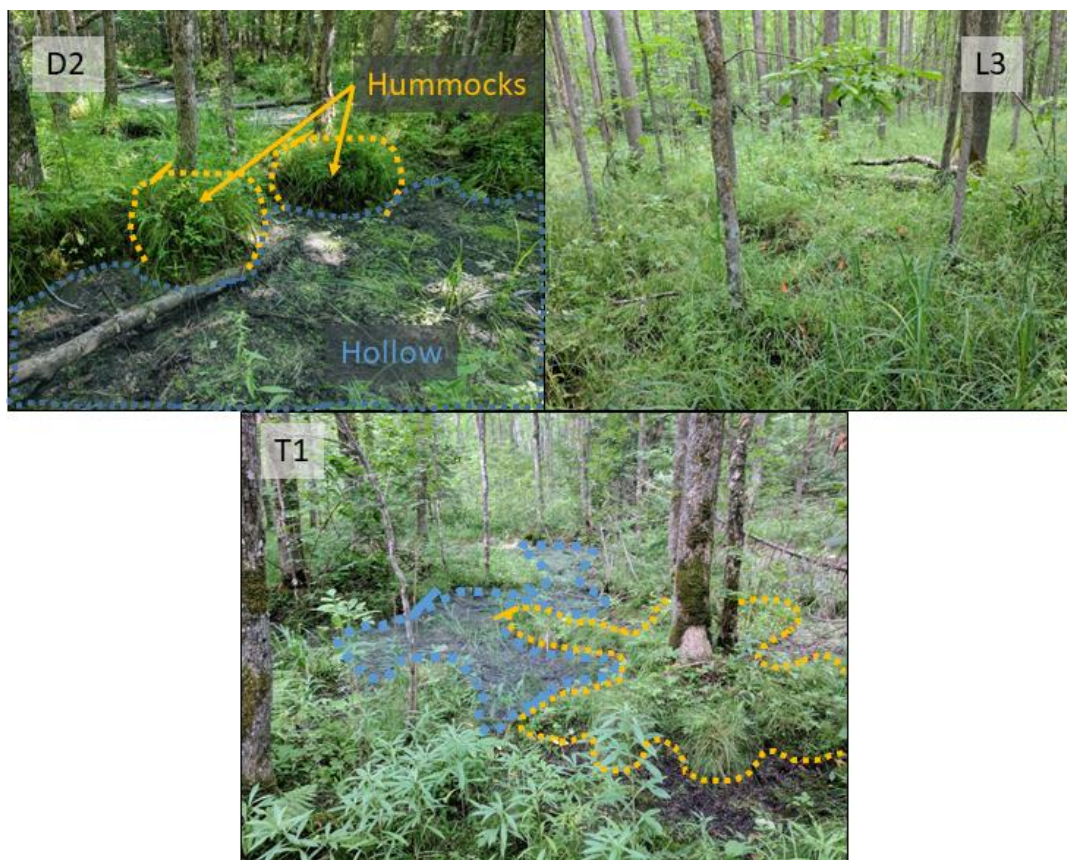


Figure 3 Photos of observed black ash wetland microtopography from a site in each hydrogeomorphic category. Hummocks are outlined in yellow/orange dashed lines, and hollows are outlined and lightly shaded in blue. Lowland site hummocks and hollows are difficult to discern in summer time due to heavy understory cover and are additionally less pronounced, so they are not drawn here.

865

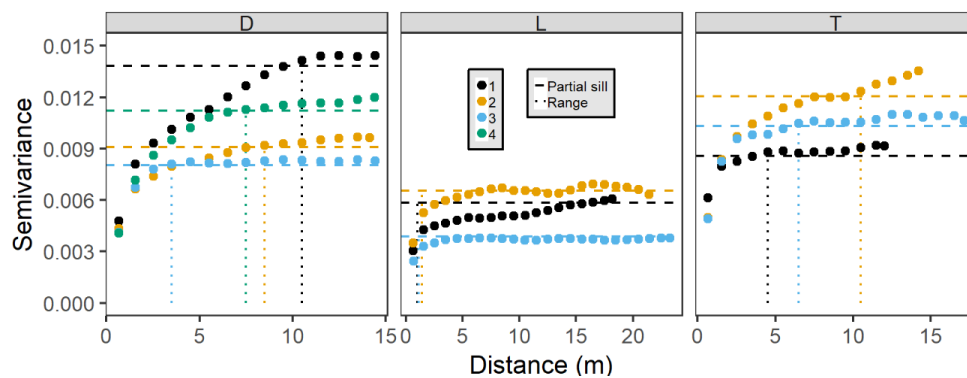
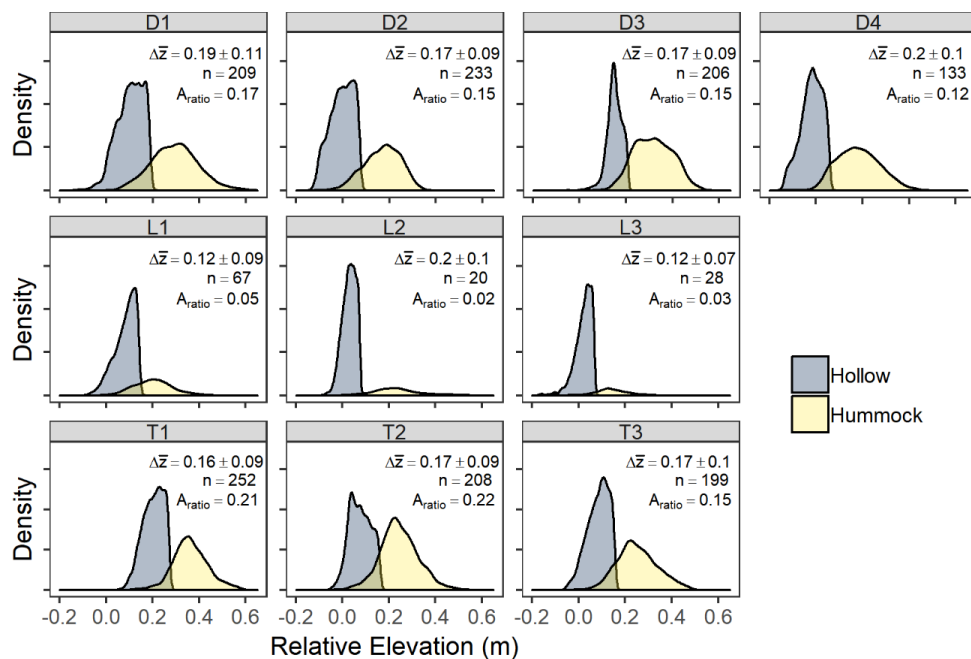
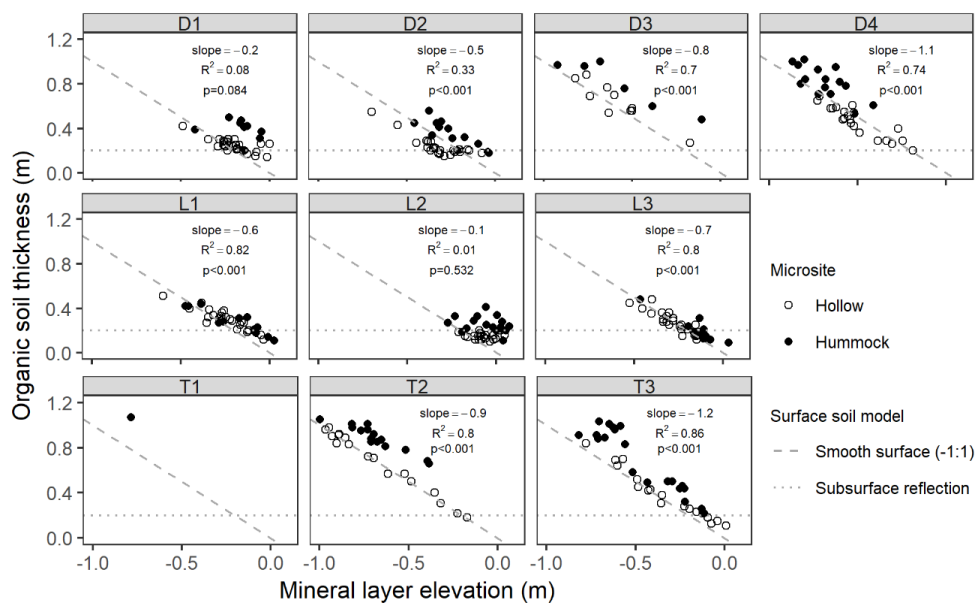


Figure 4. Omni-directional semivariograms for site elevations by hydrogeomorphic category (**D** = depression, **L** = lowland, **T** = transition). Sites are colored according to their number within their hydrogeomorphic category. Dotted vertical lines indicate best-fit ranges and horizontal dashed lines indicate best-fit partial sills (sill – nugget).



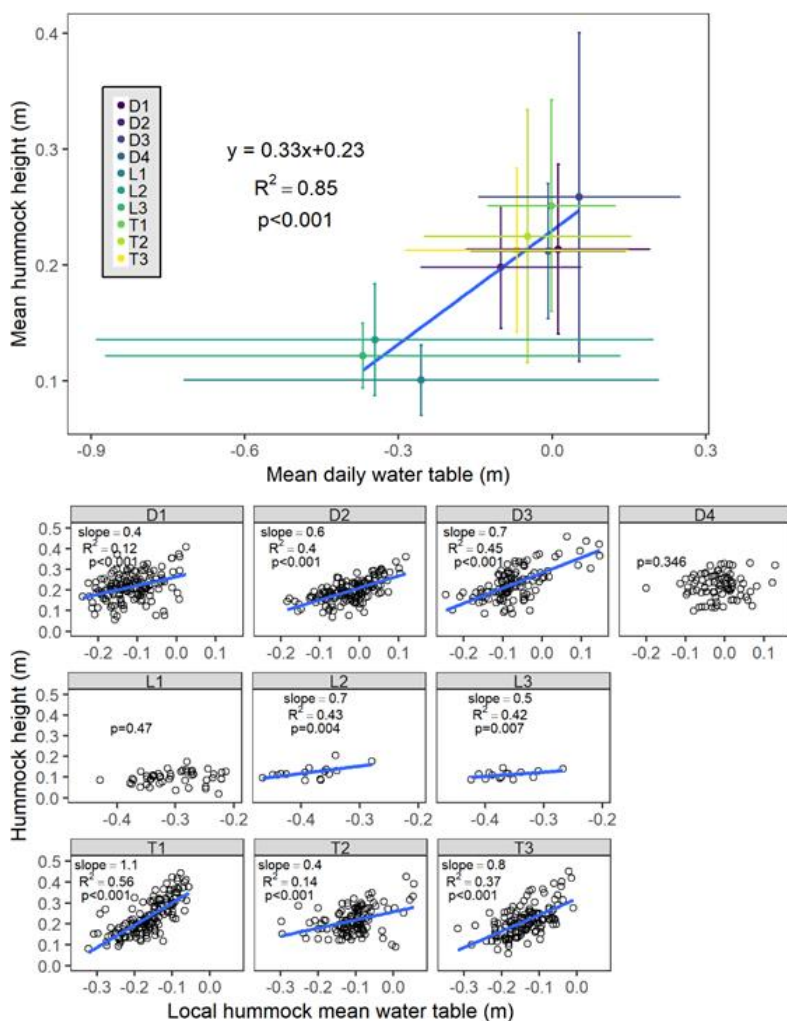
870

Figure 5. Relative elevation probability densities for each site, colored by hummock and hollow. Text indicates the difference in mean elevation ($\Delta\bar{z}$; m) between hummock and hollow at each site (\pm standard deviation), the total number of hummocks identified at each site (n), and the ratio of hummock area to total site area (A_{ratio}). Depression sites (D) occupy the top row, followed by lowland sites (L), and transition sites (T).

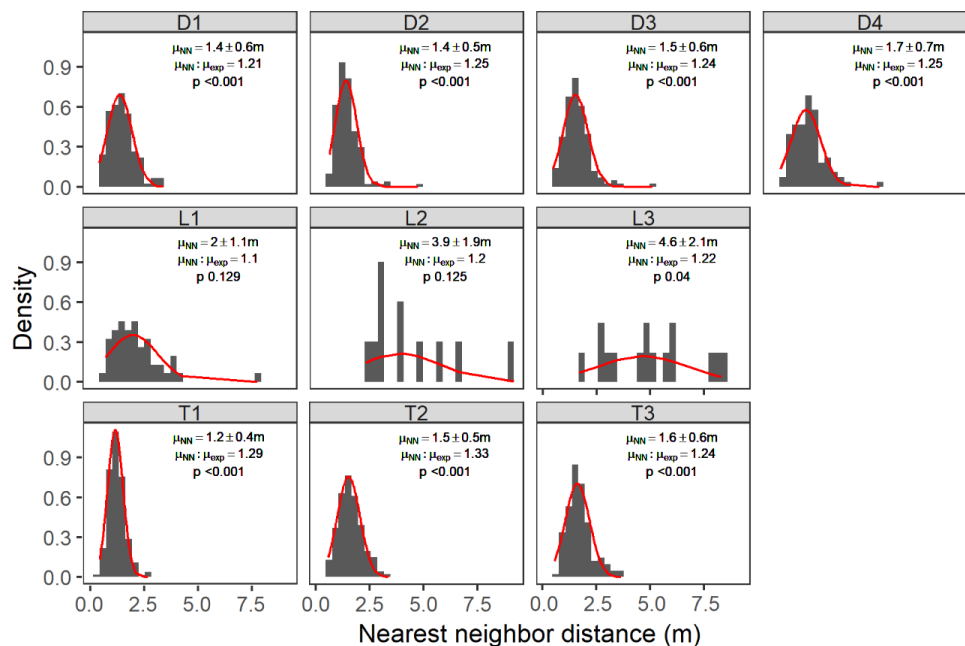


875

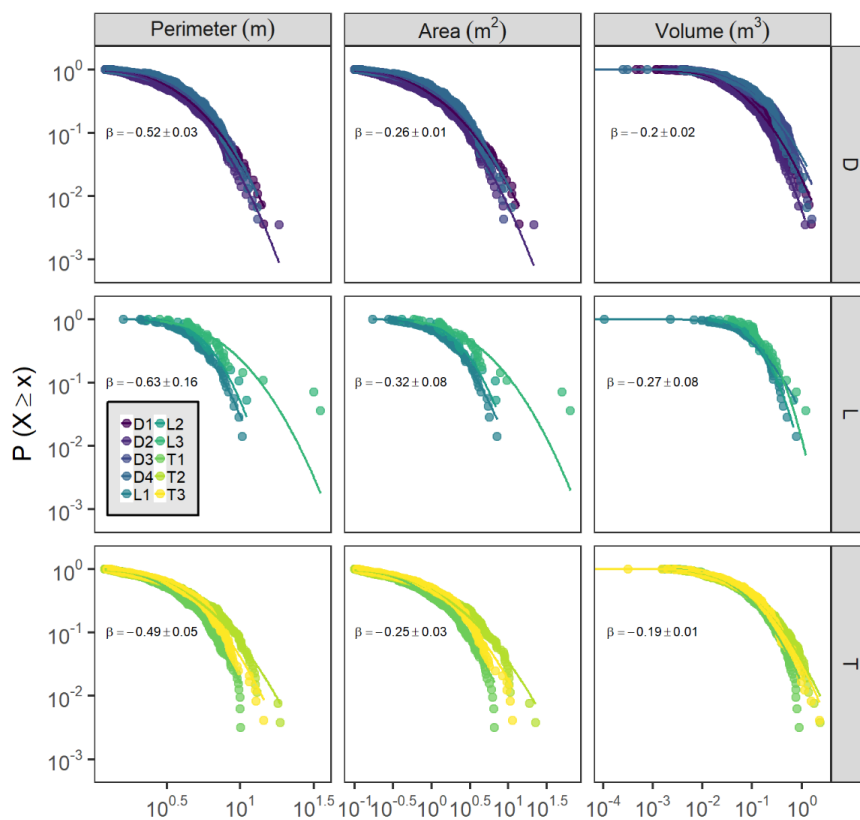
Figure 6. Organic soil thickness (measured as depth to resistance) as a function of mineral layer elevation. Points are filled by their microsite. Dashed -1:1 line indicates a smooth surface soil model and dotted horizontal line indicates a subsurface reflection model. Text values are slopes, R², and p-value of best-fit linear model for aggregated hummock and hollow points.



880 **Figure 7. Hummock height as a function of mean water table. (Top) mean site-level hummock height (\pm sd) versus mean site-level daily water table (\pm sd), and (Bottom) individual hummock height versus local daily mean water table. Slope, R^2 , and p-value for best fit linear model (blue line) presented.**



885 **Figure 8. Hummock nearest-neighbor distance distributions across sites. Bars are scaled density histograms overlain with best-fit normal distributions (red lines). Text indicates the mean nearest-neighbor distance ($\mu_{NN} \pm$ standard error); the ratio of the measured mean nearest-neighbor distance and the expected nearest neighbor distance for complete spatial randomness (μ_{exp}); and the p-value for a z-score comparison between μ_{NN} and μ_{exp} . p-values less than 0.001 indicate that hummocks are significantly overdispersed.**



890 **Figure 9.** Inverse cumulative distributions of hummock dimensions (perimeter, area, and volume) across sites (points), split by hummock dimension and site type. The y-axis is the probability that a hummock dimension value is greater than or equal to the corresponding value on the x-axis. Best-fit lognormal distributions are shown for each site as lines. All fits were highly significant ($p < 0.001$). Text indicates mean (\pm sd) within-group coefficient for a model of the form $P(X \geq x) = \beta \cdot \ln(\text{dimension_value}) + \beta_0$.